Theoretical and experimental study of the optical-absorption spectrum of exciton resonance in $In_{0.53}Ga_{0.47}As/InP$ quantum wells

Mitsuru Sugawara, T. Fujii, S. Yamazaki, and K. Nakajima
Fujitsu Laboratories, Ltd., 10-1 Morinosato-wakamiya, Atsugi-shi, Kanagawa-ken 243-01, Japan
(Received 9 April 1990; revised manuscript received 16 July 1990)

This paper presents a theoretical formulation of the integrated intensity and the profile of the optical-absorption spectrum of exciton resonance in quantum wells. Using our model, we analyzed the ground-state electron–heavy-hole exciton resonance in 20-period multiple quantum wells with 10-nm $In_{0.53}Ga_{0.47}As$ wells and 10-nm InP barriers. We found the intrinsic integrated intensity in this quantum well to be 1.1×10^{-4} eV, which was about 70% of that in $GaAs/Al_{0.25}Ga_{0.75}As$ quantum wells reported by Masselink. We demonstrate quantitatively that the smaller integrated intensity is due to the larger two-dimensional exciton radius caused by the larger static dielectric constant and the smaller in-plane reduced effective mass. We propose that the resonance spectrum profile should be formed by the convolution integral between the broadening function due to the spatial inhomogeneity of exciton energy and that due to the reduction of exciton lifetime by thermal phonon scattering. Inhomogeneous broadening was found to be a Gaussian distribution from the measured low-temperature spectrum. Assuming that the LO phonon is the major scattering source for excitons and that the distribution function of their lifetime is Lorentzian with a width of half the average, we could explain the measured profile of exciton resonance up to high temperatures. We found the average exciton lifetime to be 300 fs at room temperature. We argue that inhomogeneous broadening due to composition fluctuations in $In_{0.53}Ga_{0.47}As$ wells and the larger thermal broadening due to the larger exciton-phonon coupling make the exciton spectrum broader than $GaAs/Al_{1-x}Ga_xAs$ quantum wells. We conclude that both the smaller integrated intensity and the broader spectrum make the exciton resonance in $In_{0.53}Ga_{0.47}As/InP$ quantum wells weaker. We present the condition of inhomogeneous broadening needed to observe exciton resonance at room temperature.

I. INTRODUCTION

In semiconductor quantum wells, clear optical-absorption resonance due to excitons is often observed even at room temperature. This was first found in GaAs/AlAs quantum wells by Ishibashi.[1] An exciton consists of a hole and an electron interacting through Coulomb attraction. An exciton's envelope wave function of relative motion is spherical in bulk materials.[2] In quantum wells, excitons are compressed perpendicularly toward the quantum-well layers, giving excitons a larger binding energy[3] and a stronger oscillator strength[4] than in bulk, and making their optical-absorption spectra easier to observe at room temperature. Spectra around the absorption edge have a steplike continuum and two resonance spectra:[5] one assigned to an electron–heavy-hole (HH) and one to an electron–light-hole (LH) exciton transition. The electron-HH exciton spectrum is at the absorption edge, and the electron-LH exciton spectrum is at a higher energy over the absorption continuum of conduction-band–to–HH-valence-band transitions. This is caused by the splitting of the valence band at the Γ point due to quantum confinement.[6]

Two remarkable optical characteristics have been found in this enhanced exciton resonance. The first is the electric-field-induced shift of exciton resonance toward lower energies. This is called the quantum confined Stark effect.[7] When the electric field is perpendicular to the quantum-well layers, the exciton resonance remains clearly up to about 10^5 V/cm because the potential barriers prevent the ionization of excitons. The other optical characteristic is the large optical nonlinearity[8] caused by the excited high-density electron-hole plasma including excitons or, in a broad sense, by electrically injected carriers. The origin of this nonlinearity is understood in terms of the exclusion principle and the screening of Coulomb attraction.[9–11] Both of these optical effects make it possible to modulate dielectric constants much more than in bulk materials. They are useful for developing new devices such as high-speed optical modulators,[12] optical switches,[13] optical bistable devices [self-generated electro-optic effect devices (SEED's)],[14] etalon-type optical bistable devices,[15] and bistable lasers.[16]

The stronger the exciton resonance, the better the performance of these devices. The intensity of the ground-state electron-HH exciton resonance is especially important since it is located at the absorption edge. So far, experimental studies show that the optical-absorption coefficient of the exciton resonance depends on the material that makes up the quantum-well structure. In a 9.6-nm $GaAs/Al_{0.28}Ga_{0.72}As$ quantum well, Chemla[17] reported an optical-absorption coefficient of about 1.2×10^4 cm^{-1} at the electron-HH exciton resonance peak at room temperature. Iwamura[18] showed the resonance to be

about 1.6×10^4 cm^{-1} at 296 K in a 9.5-nm GaAs/AlAs quantum well. In our previous papers, we have shown the resonance in $In_{0.53}Ga_{0.47}As/InP$ and $In_{0.58}Ga_{0.42}As_{0.9}P_{0.1}/InP$ quantum wells, which are very promising for use in 1-μm region optical communication systems.[19–21] We found that the room-temperature absorption coefficient at the electron-HH exciton resonance peak was around $(7-8)\times10^3$ cm^{-1}, when wells were 10 nm thick. Weiner[22] showed the absorption coefficient to be about 4×10^3 cm^{-1} in 11-nm $In_{0.53}Ga_{0.47}As/In_{0.52}Al_{0.48}As$ quantum wells. Bar-Joseph[23] reported an identical absorption coefficient in 10-nm $In_{0.53}Ga_{0.47}As/InP$ quantum wells. These values are about half of our results, which is probably because they took the total thickness of well and barrier layers as light-absorbing region in processing the transmission data, while we took the thickness of only the well layers. In general, long-wavelength quantum wells such as $In_{1-x}Ga_xAs_yP_{1-y}/InP$ (Refs. 19–21 and 23–25), $In_{0.53}Ga_{0.47}As/In_{0.52}Al_{0.48}As$ (Refs. 22, 26, and 27), and $GaSb/Al_{1-x}Ga_xSb$ (Ref. 28) quantum wells show weaker exciton resonance than $GaAs/Al_{1-x}Ga_xAs$ quantum wells. The room-temperature exciton resonance occasionally merged into the band-to-band absorption continuum, and could not be detected.[19] The cause for this weaker exciton resonance is not well understood probably because there has been no intensive and quantitative study on exciton resonance spectrum.

The purpose of this work is to explain this experimental result and, more generally, to develop a comprehensive understanding of exciton resonance in quantum wells. We studied the optical-absorption spectra of electron HH exciton resonance in $In_{0.53}Ga_{0.47}As/InP$ quantum wells both experimentally and theoretically. First, we discuss the theoretical model of the integrated intensity and the profile of exciton resonance spectrum. Based on our model, we then analyze the measured spectra in $In_{0.53}Ga_{0.47}As/InP$ multiple quantum wells (MQW's) grown by low-pressure metalorganic vapor-phase epitaxy (MOVPE). We demonstrate that this quantum well has smaller integrated intensity than $GaAs/Al_{1-x}Ge_xAs$ quantum wells due to the larger two-dimensional exciton radius, and a broader spectrum due to composition fluctuations in $In_{0.53}Ga_{0.47}As$ wells and a larger exciton LO phonon coupling, showing weaker exciton resonance. We present the condition of inhomogeneous broadening needed to observe exciton resonance at room temperature in $In_{0.53}Ga_{0.47}As/InP$ quantum wells.

II. THEORETICAL MODEL OF EXCITON SPECTRUM

According to the time-dependent perturbation theory, the optical absorbance of exciton resonance in a quantum well is given by

$$\alpha_{ex}L_{QW}=SB(\hbar\omega-E_{ex}) , \tag{1}$$

where

$$S=\frac{\pi e^2\hbar}{\epsilon_0 cnm_0^2E_{ex}D}\left|\langle\varphi_e(z)|\varphi_h(z)\rangle\sum_{\mathbf{k}_\parallel}A(\mathbf{k}_\parallel)P_{cv}\right|^2 \tag{2}$$

is the integrated intensity of the exciton spectrum based on the effective-mass approximation[29–31] and $B(\hbar\omega-E_{ex})$ is the normalized broadening function. Taking the period in a MQW structure as L_{QW}, α_{ex} represents the average optical-absorption coefficient of a quantum well. The integrated intensity is proportional to the creation rate of excitons (the oscillator strength of exciton transitions). The absorbance of the exciton resonance peak is proportional to the integrated intensity and roughly proportional to the inverse of the width of the broadening function. Thus, to understand the characteristics of exciton resonance, we need to understand both the integrated intensity and the broadening function. We begin by deriving a formula for the integrated intensity explicitly including material parameters of quantum wells based on Eq. (2). To our knowledge, the analytical expression of Eq. (2) has not been presented. Previous reports discussed only the width of the broadening function. We propose a model to describe the entire spectrum profile at any temperature.

A. Integrated intensity

In Eq. (2), e is the charge of an electron, $\hbar$ is Planck's constant divided by 2π, ϵ_0 is the permittivity of a vacuum, c is the speed of light, n is the refractive index, m_0 is the mass of an electron, and D is the area of the quantum well. P_{cv} is the optical matrix element between the conduction-band and the valence-band Bloch states. E_{ex} is the exciton energy given by $E_{ex}=E_g+E_e+E_h-E_B$, where E_g is the band gap of the well material, E_e is the confined electron energy, E_h is the confined hole energy, and E_B is the exciton binding energy. An exciton state is formed by the linear combination of the product of single-particle Bloch state in the conduction and valence bands. $A(\mathbf{k}_\parallel)$ is its expansion coefficient at the in-plane wave vector $\mathbf{k}_\parallel$, and it is given by the Fourier transform of the in-plane exciton envelope wave function.

The envelope wave function of excitons in quantum wells is given by[7]

$$\Phi=\frac{1}{\sqrt{D}}e^{i\mathbf{K}\cdot\mathbf{R}}\varphi_e(z_e)\varphi_h(z_h)\phi_{ex}(\mathbf{r}) , \tag{3}$$

where $\varphi_e(z_e)$ is the electron envelope wave function describing a confined state, $\varphi_h(z_h)$ is that of the hole, and $\phi_{ex}(r)$ represents the relative in-plane motion of an electron and a hole. z_e is the coordinate of an electron in the direction perpendicular to quantum-well layers, z_h is the coordinate of the hole, $\mathbf{r}$ is their relative in-plane distance, $\mathbf{R}$ is the in-plane center of mass of an electron and a hole, and $\mathbf{K}$ is the wave vector of its motion. We assumed that the Coulomb attraction is weak compared to the quantum confinement effect, and that the confined-state wave functions are not perturbed by the Coulomb attraction. Based on the finite square potential model,[32] the electron wave function can be calculated using the conduction-band discontinuity ΔE_c, and the hole wave function can be calculated using the valence-band discontinuity ΔE_v. We take[7]

$$\phi_{ex}(\mathbf{r})=\left[\frac{2}{\pi}\right]^{1/2}\frac{1}{\lambda_{ex}}e^{-r/\lambda_{ex}}, \tag{4}$$

where λ_{ex} is the two-dimensional exciton radius.

$A(\mathbf{k}_{\parallel})$ can be written as

$$A(\mathbf{k}_{\parallel})=\frac{1}{\sqrt{D}}\int d^2\mathbf{r}\, e^{-i\mathbf{k}_{\parallel}\cdot\mathbf{r}}\phi_{ex}(\mathbf{r})\delta_{\mathbf{K},0} \tag{5a}$$

$$=\left[\frac{8\pi}{D}\right]^{1/2}\frac{\lambda_{ex}}{(1+k_{\parallel}^2\lambda_{ex}^2)^{3/2}}. \tag{5b}$$

We omitted $\delta_{\mathbf{K},0}$ in Eq. (5b). The integration in Eq. (5a) was done by Schmitt-Rink.[11] We can see that the contribution to $A(\mathbf{k}_{\parallel})$ in Eq. (2) is negligible when $k_{\parallel}\gg 1/\lambda_{ex}$. Since λ_{ex} is around 10 nm (refer to the calculation of λ_{ex} in 9.5-nm $GaAs/Al_{0.32}Ga_{0.68}As$ quantum wells by Miller[7]), we can take the value of P_{cv} at band edge. The summation in $\mathbf{k}_{\parallel}$ space, A, is given by

$$A=\sum_{\mathbf{k}_{\parallel}}A(\mathbf{k}_{\parallel})=\sqrt{D}\,\phi_{ex}(0). \tag{6}$$

The integrated intensity can be written as

$$S=\frac{4e^2\hbar|P_{cv}|^2}{\epsilon_0 cnm_0^2E_{ex}\lambda_{ex}^2}|\langle\varphi_e(z)|\varphi_h(z)\rangle|^2. \tag{7}$$

Note that degeneracy due to spin is taken into account.

The two-dimensional exciton radius can be determined by a variational method to maximize the exciton binding energy of[7]

$$E_B(\lambda_{ex})=-\frac{\hbar^2}{2\mu\lambda_{ex}^2}+\frac{e^2}{4\pi\epsilon}\left\langle\Phi\left|\frac{1}{\rho}\right|\Phi\right\rangle, \tag{8}$$

where μ is the reduced effective mass parallel to the quantum-well layers given by $(1/m_e+1/m_h^{\parallel})$, $m_h^{\parallel}$ is the effective mass of holes in that direction, m_e is the electron effective mass, ϵ is the static dielectric constant, and $\rho=[r^2+(z_e-z_h)^2]^{1/2}$.

The optical matrix element at the band edge is given by

$$|P_{cv}|^2=|\langle u_c|\mathbf{e}\cdot\mathbf{p}|u_v\rangle|^2=M_{QW}M^2, \tag{9}$$

where u_c is the Bloch function at the conduction-band edge and u_v is the Bloch function at the valence-band edge. M is the average matrix element for Bloch states given by[33]

$$M^2=\frac{m_0^2E_g(E_g+\Delta)}{12m_e(E_g+\frac{2}{3}\Delta)}, \tag{10}$$

where Δ is the spin orbit splitting energy of the valence bands. M_{QW} is the polarization factor and is $\frac{3}{2}$ for electron-HH transition and $\frac{1}{2}$ for electron-LH transition at absorption edges when the polarization vector $\mathbf{e}$ is parallel to the quantum-well layers.[34]

Equation (8) shows that the smaller the static dielectric constant, and the larger the reduced effective mass, the larger the exciton binding energy. This gives a smaller exciton radius, and thus a larger integrated intensity given by Eq. (7). Equation (10) shows that the integrated intensity is also proportional to the inverse of the electron effective mass. Note that E_{ex} in Eq. (7) and E_g in Eq. (10) almost cancel.

The integrated intensity in three-dimensional (3D) bulk material S_{3D} can be obtained by using $A=\sqrt{V}\,\phi_{ex}(0)$ and eliminating $\langle\varphi_e(z)|\varphi_h(z)\rangle$ in Eq. (2) and M_{QW} in Eq. (9). To compare the intensity with that of a quantum well, we suppose a bulk with the same volume as a quantum well: $V=L_{QW}D$. The three-dimensional exciton envelope wave function of the relative motion is given as $\phi_{ex}(r)=1/(\pi a_0^3)^{1/2}\exp(-r/a_0)$, where a_0 is the three-dimensional exciton radius. Thus, the ratio between S and S_{3D} can be written as

$$S/S_{3D}=\frac{2|\langle\varphi_e|\varphi_h\rangle|^2a_0^3M_{QW}}{\lambda_{ex}^2L_{QW}}. \tag{11}$$

Equation (11) tells us how much the integrated intensity is increased as we go from three- to two-dimensional system.

B. Broadening function

The exciton spectrum broadening at low temperatures is primarily due to the spatial inhomogeneity of the exciton energy level caused by structural imperfections in the quantum wells, such as interface roughness,[36] composition fluctuations in constituent alloys,[19–21,37] and nonperiodicity in multiple quantum wells.[21] Excitons, once created by photon absorption, are ionized to free electron-hole plasma by phonon scattering (under an electric field, ionization by tunneling through the barriers on the opposite sides must be also taken into account). At high temperatures, the density of phonons increases, reducing the exciton lifetime[38] and further broadening the spectrum according to the uncertainty principle.

Temperature dependence of exciton spectrum width Γ has been studied experimentally in $GaAs/Al_{1-x}Ga_xAs$ quantum wells,[8,17,18] in $In_{0.53}Ga_{0.47}As/In_{0.52}Al_{0.48}As$ quantum wells,[23,27] and in $In_{0.53}Ga_{0.47}As/InP$ quantum wells.[39] In all reports, the spectrum broadening was analyzed by the linear combination of the inhomogeneous broadening width Γ_0 and the thermal broadening width $\Gamma_T(T)$:

$$\Gamma=\Gamma_0+\Gamma_T(T). \tag{12}$$

Here, LO phonon scattering was assumed to be a major source of thermal broadening:

$$\Gamma_T(T)=\frac{\Gamma_{ph}}{\exp(\hbar\omega_{LO}/k_BT)-1}, \tag{13}$$

where $\hbar\omega_{LO}$ is the LO-phonon energy, and Γ_{ph} is the coupling constant with excitons.

However, we must note that the cause of the inhomogeneous and thermal broadening is principally different in the sense that Γ_0 represents the spatial inhomogeneity of the exciton energy and Γ_T represents the uncertainty in measuring the energy of the exciton resonance. The exciton energy level depends on the sites in quantum wells due to structural imperfections and each level shows thermal broadening due to scattering. Thus, we propose

that the broadening function of the exciton spectrum should be written by the convolution integral as

$$B(\hbar\omega - E_{ex}) = \int_{-\infty}^{\infty} B_0(\hbar\omega - E_{ex} + E) B_T(E) dE \ , \quad (14)$$

where B_0 is the broadening function due to the inhomogeneity of the exciton energy and B_T is that due to the uncertainty in the exciton energy depending on the exciton lifetime. We assume that the exciton lifetime is independent of the slight variation in exciton energy. This is reasonable since structural imperfections primarily change the band-gap energy or quantum confinement energy, and the change in the exciton binding energy is negligible. As we showed in our last paper,[19] the low-temperature spectrum of exciton resonance is well fit to a Gaussian distribution function. Thus, we take

$$B_0(\hbar\omega - E_{ex}) = \frac{1}{\sqrt{2\pi}\xi} \exp[-(\hbar\omega - E_{ex})^2/2\xi^2] \quad (15)$$

with a full width at half maximum (FWHM) of $\Gamma_0 = 2.35\xi$. Assuming that each component of structural imperfections mentioned above occurs independently, we can deconvolute Γ_0 as[19–21]

$$\Gamma_0 = \left[\sum_i \Gamma_{0,i}^2 \right]^{1/2} , \quad (16)$$

where $\Gamma_{0,i}$ represents the FWHM of a Gaussian broadening function due to each structural imperfection.

According to the time-dependent perturbation theory,[40] the resonance spectrum between discrete levels broadens by $(1/\pi b)\sin^2(E/b)/(E/b)^2$ within a finite observation time of $t = 2\hbar/b$. The FWHM of this function is $5.56\hbar/t$. As t increases, this function approaches a δ function. The exciton resonance spectrum broadens according to this function with t as the exciton lifetime τ. Thus, B_T can be described as

$$B_T(E) = \int_0^{\infty} \frac{f(\tau)}{\pi b} \frac{\sin^2(E/b)}{(E/b)^2} d\tau \ , \quad (17)$$

where $f(\tau)$ represents the normalized distribution function of exciton lifetime and $b = 2\hbar/\tau$. In Sec. IV, we show that the profile of the measured spectrum can be explained well using a Lorentzian distribution as $f(\tau)$.

The measured FWHM of the ground-state electron-HH exciton spectra in III-V-compound semiconductor quantum wells is comparable to the exciton binding energy. Chemla[17] reported room-temperature exciton spectrum with about 7.5-meV FWHM in 9.6-nm $GaAs/Al_{0.28}Ga_{0.72}As$ quantum wells. Green[3] calculated the exciton binding energy as 8 meV in $GaAs/Al_{0.3}Ga_{0.7}As$ quantum wells when wells are 10 nm. Thus, the higher energy side of the electron-HH exciton spectrum at the absorption edge is not completely separated from the absorption continuum due to band-to-band transitions. As the spectrum broadens, the exciton resonance gradually merges into the continuum. The optical absorbance of the band-to-band transition can be written as[41]

$$\alpha_c L_{QW} = \frac{\pi e^2 \hbar |P_{cv}|^2}{\epsilon_0 c n m_0^2 \hbar\omega} |\langle \varphi_e(z) | \varphi_h(z) \rangle|^2 F_s(\hbar\omega) J_{cv} \ , \quad (18)$$

where $J_{cv} = \mu/\pi\hbar^2$ represents the joint density of states per unit area between conduction and valence bands, and $F_s(\hbar\omega)$ is the Sommerfeld factor.[17,42] The Sommerfeld factor describes an increase in the band-to-band optical absorption due to the Coulomb interaction, which is equal to 2 at the absorption edge. The ratio of the average optical-absorption coefficient at the exciton resonance peak and the continuum is given by

$$\alpha_{ex}/\alpha_c = 1.88 \frac{\hbar^2}{\Gamma \lambda_{ex}^2 \mu} \ . \quad (19)$$

Here, we canceled E_{ex} in Eq. (7) and $\hbar\omega$ in Eq. (18) and assumed that the exciton resonance obeys a Gaussian distribution. the value of α_{ex}/α_c represents a contrast of exciton resonance against the band-to-band continuum.

III. EXPERIMENT

We grew $In_{0.53}Ga_{0.47}As/InP$ MQW's on (100)-oriented InP substrates by low-pressure MOVPE. Three samples (samples I, II, and III) were grown by the horizontal-type reactor, in which we grew $In_{0.58}Ga_{0.42}As_{0.9}P_{0.1}/InP$ quantum wells reported in Ref. 21. The growth temperature was around 600 °C. We first grew a 100-nm undoped InP buffer layer on an InP substrate, and then a 20-period undoped MQW consisting of about 10-nm $In_{0.53}Ga_{0.47}As$ wells and 10-nm InP barriers. The background electron concentration is around 1×10^{15} cm^{-3}. The In, Ga, As, and P sources were trimethyleindium, triethylegallium, arsine, and phosphine. Pd-diffused high-purity hydrogen was the carrier gas. The total carrier-gas flow rate was six standard liters per minute. The growth rate of MQW layers was about one monolayer per second.

The thickness of well and barrier layers in a period of MQW's was determined by analyzing small-angle x-ray diffraction patterns. Figure 1(a) shows the diffraction pattern of sample II with the x-ray incident angle from $\theta = 0.3°$ to 2.0°. Up to seventh order, interference peaks due to the periodic structure of the MQW are observed. We used a computer-controlled Rigaku small-angle diffractometer with Cu $K\alpha$ radiation. The experimental setup was described in Refs. 43 and 44. In these papers, we showed that the structure of MQW's can be uniquely determined by analyzing the first and secondary diffraction peaks based on optical multilayer theory. In Fig. 1(b), circles represent the measured diffraction patterns around the first and secondary (hardly observed) peaks. The lines show the calculated diffraction pattern when the $In_{0.53}Ga_{0.47}As$ well is 9.8 nm and the InP barrier is 9.6 nm that agrees best with the measurements. The reflectivity of the measured pattern is adjusted to the calculation of the first-order peak. The even order peaks are hardly observed because the well and barrier thicknesses are almost equal. Error is estimated within 0.2 nm. The well thickness determined using the same procedure was 10.3 nm and the barrier thickness 9.4 nm in sample I. The well was 9.9 nm and the barrier was 9.8 nm in sample III.

We measured the optical absorption spectra of the MQW's from 4.2 to 380 K. Samples were immersed in

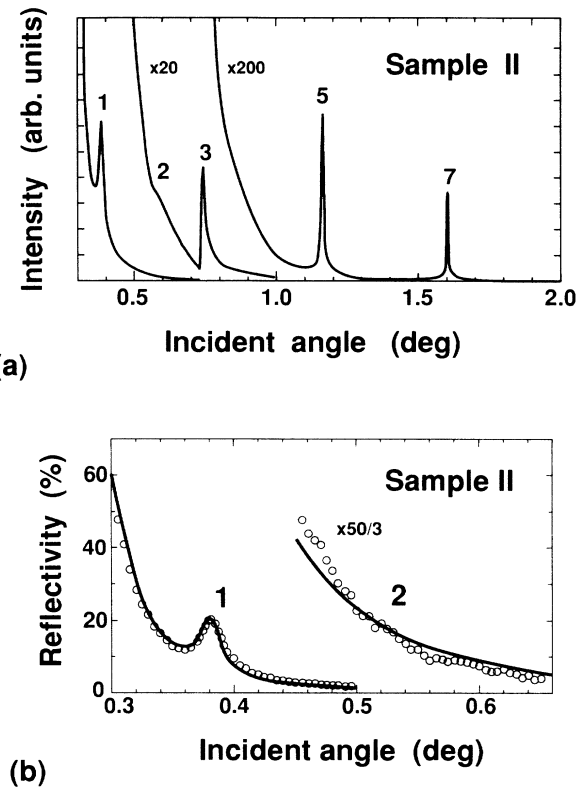

FIG. 1. (a) X-ray diffraction pattern of sample II with an incident angle from 0.3° to 2.0°. The order of the interference peaks is also shown. (b) X-ray diffraction pattern around the first- and the second-order (hardly observed) interference peaks. The circles represent the measured pattern. The lines represent calculations based on optical multilayer theory when $In_{0.53}Ga_{0.47}As$ wells are 9.8 nm and InP barriers are 9.6 nm. The reflectivity of the measured pattern is adjusted to the calculation at the first-order peak.

liquid helium at 4.2 K. Between 9 and 380 K, we used a cryostat built by Technolo Industry, Ltd. Temperature at the sample was controlled by a helium refrigerator and a PID-controlled heater. A beam from a halogen lamp dispersed by a 0.32-m single-pass monochrometor was focused to a diameter of 250 μm on the MQW samples. Here, the polarization vector in Eq. (9) is parallel to the quantum-well layers, giving $M_{QW}=\frac{3}{2}$ for electron-HH exciton transition. The light transmitted through the sample was detected by a PbS detector using a conventional lock-in technique. The ratio between the intensity of the light transmitted from a sample, I_1, and an InP substrate, I_2, was normalized to one at an energy below the absorption edge where optical absorption by a MQW could be neglected. The optical absorbance of one quantum well was determined by $\alpha L_{QW}=(1/N)\ln(I_2/I_1)$, where I_1 and I_2 are the light transmitted from a sample and from an InP substrate, and N is the number of the wells. Since 10-nm InP barrier layers are thick enough to neglect the interference of confined-state wave functions, Eq. (2) derived for a single quantum well holds in our MQW's.

IV. EXCITON RESONANCE IN $In_{0.53}Ga_{0.47}As/InP$ QUANTUM WELLS

In this section, we show the measured optical-absorption spectra of the $In_{0.53}Ga_{0.47}As/InP$ MQW's and analyze the spectra based on the model we presented in Sec. II.

Figure 2 shows the measured optical-absorption spectra of sample I. The vertical axis is described by the absorbance of a quantum well. The absorption edge shifted toward longer wavelengths as temperature increased due to the decreased $In_{0.53}Ga_{0.47}As$ band gap. We can observe resonance spectra of the ground-state electron-HH and -LH excitons over the steplike absorption continuum. (Only electron-HH resonance is shown in Fig. 2, except at 4.2 K.) The exciton spectrum decreases in the absorbance and merges into a continuum as temperature increases. Taking the peak of the spectra as the exciton energy and using the low-energy side of the spectra, we extracted the contribution of the electron-HH exciton resonance. We evaluated the integrated intensity and the profile of the spectrum as long as the absorbance at the peak is 1.2 times larger than that of the continuum to avoid errors.

Figure 3 plots the integrated intensity of electron-HH exciton resonance as a function of temperature for samples I, II, and III. The unit of the integrated intensity is written in eV. We could not find any significant difference in the integrated intensity among the three samples. The intensity remained almost constant especially below 100 K between 1.0×10^{-4} and 1.1×10^{-4} eV. Above 200 K, data is more scattered, probably due to the increasing experimental error in determining the exciton peak energy because of the broadening of the resonance spectrum. We judge the measured value to be intrinsic in $In_{0.53}Ga_{0.47}As/InP$ quantum wells, and take $S=1.1\times10^{-4}$ eV.

Stolz reported the well-width dependence of the integrated intensity measured at 5 K in $In_{0.53}Ga_{0.47}As/In_{0.52}Al_{0.48}As$ quantum wells.[26] Accord-

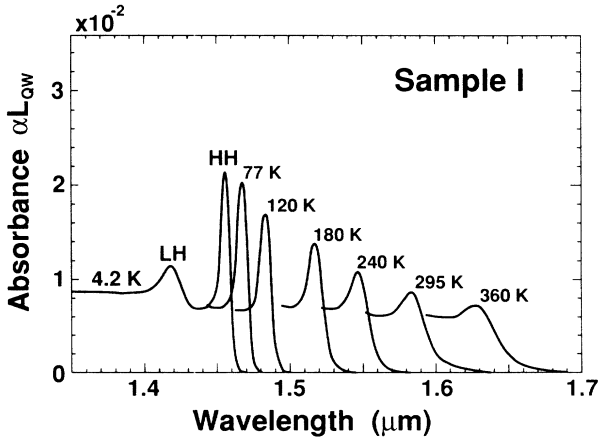

FIG. 2. Optical-absorption spectra of sample I at 4.2, 77, 120, 180, 240, 295, and 360 K. The vertical axis is the optical absorbance of a quantum well.

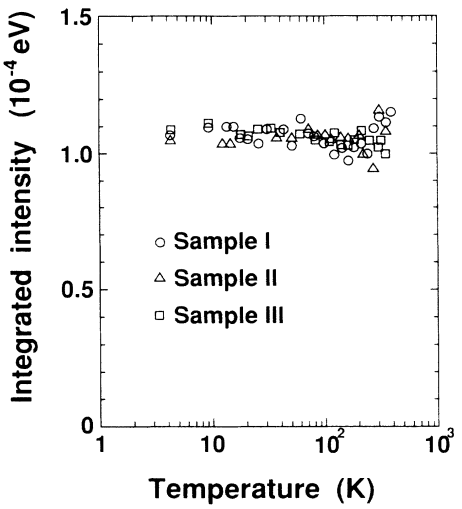

FIG. 3. Integrated intensity of the ground-state electron-HH exciton resonance as a function of temperature. Circles represent the measured values in sample I, triangles those in sample II, and squares those in sample III.

ing to Fig. 8 in Ref. 26, the integrated intensity at the well width of 10 nm seems 20% or 30% smaller than our value. The reason for this discrepancy is not clear. In $GaAs/Al_{0.25}Ga_{0.75}As$ quantum wells, Masselink[31] studied the well-width dependence of the integrated intensity below 3 K. Their data (Fig. 4 in Ref. 31) show that the integrated intensity was 160 eV/cm in 10-nm quantum wells. Considering that they used the well width to calculate the absorption coefficient from their transmission data, the integrated intensity in the absorbance spectrum is 1.6×10^{-4} eV. The integrated intensity we obtained in $In_{0.53}Ga_{0.47}As/InP$ quantum wells is about 70% of this value.

In calculating S using Eq. (7), we use the material parameters of the well layers. This is a good approximation since the exciton envelope wave function is almost confined in about 10-nm wells. We show the results of our calculation for each of the two quantum wells:

(i) $In_{0.53}Ga_{0.47}As/InP$ quantum wells: Using $E_g=0.75$ eV and $\Delta=0.35$ eV at 300 K and $m_e=0.041m_0$, we obtain $|P_{cv}|^2=3.41m_0E_g$ from Eqs. (9) and (10). We calculated $\varphi_e(z)$ and $\varphi_h(z)$ assuming that ΔE_c was 40% of the band-gap difference, ΔE_g, between InP and $In_{0.53}Ga_{0.47}As$,[45] and obtained $\langle\varphi_e(z)|\varphi_h(z)\rangle=0.96$. [The integration over well layers is $\langle\varphi_e(z)|\varphi_e(z)\rangle_{\text{well}}=0.95$ and $\langle\varphi_h(z)|\varphi_h(z)\rangle_{\text{well}}=1.0$, confirming that excitons are almost confined in wells.] Since the calculated quantum energy level was $E_e+E_h=45$ meV, E_g/E_{ex} is evaluated to be 0.95. Using $n=3.6$, we obtain

$$S=2.32\times10^{-2}/(\lambda_{\text{ex}}[\text{nm}])^2\ \text{eV}\ , \tag{20}$$

where λ_{ex} is in nm. Substituting $S=1.1\times10^{-4}$ eV, we obtain $\lambda_{\text{ex}}=14.5$ nm.

(ii) $GaAs/Al_{0.25}Ga_{0.75}As$ quantum wells: We use $E_g=1.424$ eV and $\Delta=0.34$ eV at 300 K, $m_e=0.068m_0$, $\Delta E_c=0.57\Delta E_g$, and $n=3.6$. $\langle\varphi_e(z)|\varphi_h(z)\rangle$ was calculated to be 0.99. ($\langle\varphi_e(z)|\varphi_e(z)\rangle_{\text{well}}=0.96$ and $\langle\varphi_h(z)|\varphi_h(z)\rangle_{\text{well}}=0.99$, confirming that excitons are almost confined in wells.) We obtained

$$S=1.49\times10^{-2}/(\lambda_{\text{ex}}[\text{nm}])^2\ \text{eV}\ . \tag{21}$$

Substituting $S=1.6\times10^{-4}$ eV, we obtain $\lambda_{\text{ex}}=9.7$ nm. Thus, the smaller integrated intensity in $In_{0.53}Ga_{0.47}As/InP$ quantum wells is due to the larger two-dimensional exciton radius.

The two-dimensional exciton radius is related to the static dielectric constant and the in-plane reduced effective mass as can be seen in Eq. (8). We use the static dielectric constant of bulk layers: $\epsilon=13.9\epsilon_0$ for $In_{0.53}Ga_{0.47}As$ (Ref. 46) and $\epsilon=12.5\epsilon_0$ for GaAs.[47] The in-plane reduced effective mass is not well defined, however. The Luttinger parameters of $\gamma_1=11.01$ and $\gamma_2=4.28$ derived for $In_{0.53}Ga_{0.47}As$ by Alavi[48] gives $m_h^{\parallel}=m_0/(\gamma_1+\gamma_2)=0.065m_0$, and thus $\mu=0.025m_0$ using $m_e=0.041m_0$. Stolz[49] experimentally obtained $\mu=0.051m_0$ from the magnetoabsorption measurements in 8.0-nm $In_{0.53}Ga_{0.47}As/In_{0.52}Al_{0.48}As$ MQW's, which is about twice as large as the theoretically predicted value. They attributed this enhancement to the increased electron effective mass due to the nonparabolicity of the $In_{0.53}Ga_{0.47}As$ conduction band and/or the much heavier heavy-hole mass caused by the mixing of split valence bands. Based on Eq. (8), $\lambda_{\text{ex}}=14.5$ nm and $\epsilon=13.9\epsilon_0$ gives $\mu=0.04m_0$ (and a binding energy of 6.6 meV). This value, being between the above mentioned theoretical and experimental values, is reasonable. For $GaAs/Al_{0.25}Ga_{0.75}As$ quantum wells, Eq. (8) with $\lambda_{\text{ex}}=9.7$ nm and $\epsilon=12.5\epsilon_0$ is satisfied by $\mu=0.061m_0$ (exciton binding energy was 10.5 meV), which is about 1.5 times larger than in $In_{0.53}Ga_{0.47}As/InP$ quantum wells. Thus, the larger two-dimensional exciton radius in $In_{0.53}Ga_{0.47}As/InP$ quantum wells can be attributed to the larger static dielectric constant and the smaller in-plane reduced effective mass.

Now, we can evaluate how much the integrated intensity is increased in quantum wells compared with bulk materials. The effective-mass equation for the three-dimensional exciton problem can be solved analytically,[2] giving $a_0=0.053(m_0/\mu)(\epsilon/\epsilon_0)$ (in nm). Using $\epsilon=13.9\epsilon_0$ and $\mu=0.038m_0$ for bulk $In_{0.53}Ga_{0.47}As$, we obtain $a_0=19.3$ nm. Using $\epsilon=12.5\epsilon_0$ and $\mu=0.056m_0$ for bulk GaAs, we obtain $a_0=11.8$ nm. In MQW's with 10-nm wells and 10-nm barriers, the ratio S/S_{3D} can be calculated setting $L_{\text{QW}}=20$ nm in Eq. (11). In $In_{0.53}Ga_{0.47}As/InP$ quantum wells, the intensity is 4.7 times greater than in bulk $In_{0.53}Ga_{0.47}As$. In $GaAs/Al_{0.25}Ga_{0.75}As$ quantum wells, the ratio is calculated to be 2.6, about half that in $In_{0.53}Ga_{0.47}As/InP$ quantum wells. The difference in the integrated intensity of exciton resonance between different materials becomes less significant as we go from a three- to a two-dimensional system. This is because the extent of the exciton wave function perpendicular to the quantum-well layers is almost restricted to the well width, independent of the materials making up the wells. In the practical application, the well width is designed to optimize the exci-

ton energy for each device. To further improve the exciton absorption behavior in quantum wells compared to bulk, we should narrow the barrier thickness to the extent that we can neglect the exciton wave-function overlap between neighboring wells. We experimentally found that the integrated intensity of exciton resonance remained constant in a MQW with barriers reduced to 6 nm.

Figure 4 shows the measured optical-absorption spectra at 4.2 and 295 K. At 4.2 K, the electron-HH exciton resonance spectrum has a Gaussian distribution of B_0 with $\Gamma_0=4.7$ meV. At 295 K, we assumed that the distribution function of exciton lifetime is Lorentzian with an average lifetime of 300 fs and a FWHM of half the average (150 fs). The calculated curve explains the profile of the measure electron-HH exciton resonance well. The 295-K profile has a longer tail than the profile at 4.2 K. The tail does not fit to a Gaussian distribution. We could not experimentally determine the spectrum profile where the absorbance is less than 10^{-4} since the transmission is almost equal to one in our 20-period MQW's.

Figure 5 shows the FWHM of the electron-HH exciton spectrum as a function of temperature for the three samples. Data is plotted as long as exciton resonance is 1.2 times larger than the continuum. The inhomogeneous broadening was $\Gamma_0=6.0$ meV in sample II and $\Gamma_0=8.5$ meV in sample III, both larger than in sample I. The spectrum broadened as temperature increased, reducing the peak absorbance. The arrow at 14.6 meV is the calculated width setting $\alpha_{ex}/\alpha_c=1.2$ with $\mu=0.04m_0$ and $\lambda_{ex}=14.5$ nm in Eq. (19). This limit agrees well with measurements. We calculated the temperature dependence of the exciton spectrum width assuming that the LO phonon scattering forms a Lorentzian distribution in exciton lifetime as a major scattering source. According to Eq. (13), the temperature dependence of the average exciton lifetime is described as

$$\bar{\tau}=\tau_{ph}[\exp(\hbar\omega_{LO}/k_BT)-1] . \quad (22)$$

Equation (22) gives the lifetime of 300 fs at 295 K using $\hbar\omega_{LO}=30$ meV and $\tau_{ph}=130$ fs. The LO-phonon energy was determined from linear interpolation between 28 meV in InAs and 32 meV in GaAs reported by Soni.[50] The FWHM of the Lorentzian distribution of the exciton

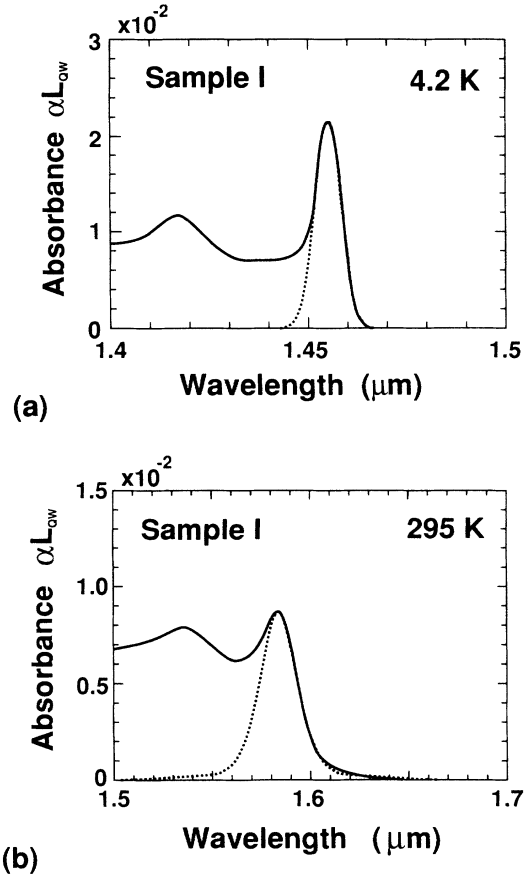

FIG. 4. (a) Optical-absorption spectrum at 4.2 K. The solid line represents measurements. The dotted line represents the Gaussian distribution of B_0 [Eq. (15)] with $\Gamma_0=4.7$ meV. (b) Optical-absorption spectrum at 295 K. The solid line represents measurements. The dotted line represents the result calculated from Eqs. (14), (15), and (17), assuming that the distribution function of exciton lifetime has a Lorentzian distribution with an average of $\bar{\tau}=300$ fs and the FWHM of half the average (150 fs).

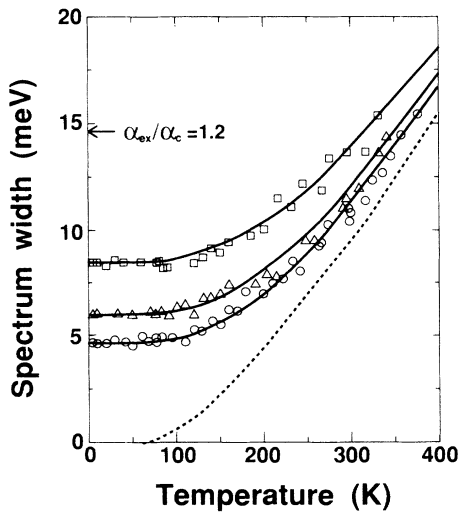

FIG. 5. Spectrum broadening (FWHM) of the ground-state electron-HH exciton resonance as a function of temperature. Circles represent the results for sample I, triangles for sample II, and squares for sample III. The arrow at 14.6 meV represents the limit to observe exciton resonance as calculated by Eq. (19) using $\mu=0.04$ and $\lambda_{ex}=14.5$ nm. The solid lines represent calculations by Eqs. (14), (15), (17), and (22), using the LO phonon energy $\hbar\omega_{LO}=30$ meV and $\Gamma_{ph}=130$ fs. We assumed that the distribution function of exciton lifetime is Lorentzian with a FWHM of half the average. The dashed line represents the contribution of thermal broadening from Eqs. (17) and (22).

lifetime was assumed to be half the average at any temperature. Calculated values for the three samples are in quite good agreement with measurements, supporting the assumption on the scattering origin. Note that the temperature dependence in the three samples with different inhomogeneous broadening can be explained by the common thermal broadening function, showing that the exciton lifetime is independent of inhomogeneous broadening. As a result, we can estimate the spectrum width at any temperature as long as we know Γ_0. The dashed line represents the FWHM of the thermal broadening function from Eq. (17). As temperature increases, the thermal broadening exceeds the inhomogeneous broadening and becomes the major factor in exciton spectrum broadening. However, note that the difference in the room-temperature spectrum width between the three samples is still caused by the difference in inhomogeneous broadening. To observe room-temperature exciton resonance by limiting the spectrum width to 14.6 meV, we need quantum wells with inhomogeneous broadening of less than about 10 meV. Our three samples meet this criteria, making exciton resonance visible at room temperature.

Now, we will discuss the origin of inhomogeneous broadening in our three samples. Inhomogeneous broadening due to composition fluctuation is characteristic in quantum wells including alloy semiconductors. Since the exciton radius is on the order of 10 nm and the number of atoms included in the exciton volume is as small as 10^5 to 10^6, excitons feel composition fluctuations statistically, resulting in inhomogeneous broadenings. Schubert[51] showed that the broadening function due to the statistical composition fluctuation obeys a Gaussian distribution with the FWHM of

$$\Gamma_{\rm sta}=2.35\left[\frac{dE_g}{dx}\right]\left[\frac{x(1-x)}{KV_{\rm 3D}}\right]^{1/2}, \tag{23}$$

where x represents the composition of alloy, $V_{\rm 3D}$ is the three-dimensional exciton volume, K is the atomic density, and dE_g/dx is the change in the band-gap energy with the composition. In bulk $In_{0.53}Ga_{0.47}As$, Eq. (23) gives $\Gamma_{\rm sta}=1.6$ meV using $V_{\rm 3D}=(4\pi/3)a_0^3$. $In_{0.53}Ga_{0.47}As$ layers grown by our MOVPE reactor typically have the Gaussian 4.2-K photoluminescence spectra with a FWHM of about 3.0 meV. We can regard the 4.2-K photoluminescence spectrum width as inhomogeneous broadening in optical-absorption spectra, since, at this low temperature, we can neglect the broadening of the Fermi-Dirac distribution function. The fact that the spectrum is broader than the calculated one shows that composition fluctuates not only statistically but also macroscopically over a several-hundred-micrometer excited area in photoluminescence measurements. To extend Schubert's formula to quantum wells, we must take into account the shrinkage of exciton volume due to quantum confinement and the spread of the exciton wave function to the binary InP barriers in very thin quantum wells. Treating the variation in the band gap as the first-order perturbation to the exciton energy, we obtain

$$\Gamma_{\rm QW}=\left[\Gamma_{\rm sta}^2\left[\frac{V_{\rm 3D}}{V_{\rm 2D}}\right]+\Gamma_{\rm mac}^2\right]^{1/2}\times\left[\left[\frac{\partial E_c}{\partial E_g}\right]\langle\varphi_e|\varphi_e\rangle_{\rm well}+\left[\frac{\partial E_v}{\partial E_g}\right]\langle\varphi_h|\varphi_h\rangle_{\rm well}\right], \tag{24}$$

where $\Gamma_{\rm mac}$ represents the contribution of macroscopic fluctuations, $V_{\rm 2D}$ is the exciton volume in quantum wells, $\partial E_c/\partial E_g$ represents the distribution of the band-gap change to the conduction band, and $\partial E_v/\partial E_g$ to the valence band. The integral is performed in well regions in the case of $In_{1-x}Ga_xAs/InP$ quantum wells. (In $GaAs/Al_{1-x}Ga_xAs$ quantum wells, the integration is done in $Al_{1-x}Ga_xAs$ barriers. When the well width is 10 nm, the integral is negligible, and so is $\Gamma_{\rm QW}$.) In 10-nm $In_{0.53}Ga_{0.47}As/InP$ quantum wells, the contribution of statistical fluctuation is calculated to be $\Gamma_{\rm QW}=3.3$ meV setting $\Gamma_{\rm mac}=0$ meV and assuming $\partial E_c/\partial E_g=0.4$ in Eq. (24). We used $V_{\rm 2D}=\pi L_W\lambda_{\rm ex}^2$, where L_W is the well width. This is the lower limit in inhomogeneous broadening in this quantum well. The magnitude of macroscopic composition fluctuations in our bulk layers is calculated to be $\Gamma_{\rm mac}=(3.0^2-1.6^2)^{1/2}=2.5$ meV. Assuming that $\Gamma_{\rm mac}$ is independent of well width, Eq. (24) gives $\Gamma_{\rm QW}=4.1$ meV setting $\Gamma_{\rm mac}=2.5$ meV. Kamei demonstrated the 4.2-K photoluminescence spectrum with a FWHM of only 3 meV in a 50-period 10-nm $In_{0.53}Ga_{0.47}As/InP$ MQW.[25] To our knowledge, this FWHM is the narrowest reported in $In_{0.53}Ga_{0.47}As$ MQW's, and is almost equal to the theoretically predicted value due to the statistical composition fluctuations, showing that his MQW has an almost perfect structure with macroscopically homogeneous composition and without other structural imperfections.

Another major component of inhomogeneous broadening is interface roughness, which causes well-width fluctuation and thus a fluctuation in quantum confinement energy. We attribute the difference in inhomogeneous broadening among our three samples to this. According to Eq. (16), the contribution of interface roughness is calculated to be 2.3 meV for sample I, 4.4 meV for sample II, and 7.4 meV for sample III using $\Gamma_{\rm QW}=4.1$ meV. We do not treat the contribution of nonperiodicity separately (e.g., the fluctuation in the average exciton energy between different wells) since the nonperiodicity in MQW's is primarily caused by interface roughness of a single quantum well, as we showed in Ref. 21. Composition fluctuation is dominant in sample I, and interface roughness in sample III.

It may be harder to obtain a smooth interface in $In_{0.53}Ga_{0.47}As/InP$ quantum wells than in $GaAs/Al_{1-x}Ga_xAs$ quantum wells because the P and As group V atoms with high vapor pressure must be completely changed at interfaces. Wang showed that $InAs_{1-x}P_x$ interface layers was formed in MOVPE growth during the growth interruption at interfaces of InP to $In_{0.53}Ga_{0.47}As$ under an arsine purge.[52] He

demonstrated this atomic substitution at interfaces studying the low-temperature photoluminescence energy of InP whose growth was interrupted by an arsine purge. The As composition increased with purge time and arsine flow rate. This interface layer will decrease the quality of interface partly because the substitution will occur inhomogeneously and partly because defects will be incorporated due to the strain. Kamei[25] shortened the time for growth interruption to 0.5 seconds to prevent the substitution, and obtained high-quality interfaces. We suppose that his vertical-type MOVPE reactor is designed to prevent convection and enables the fast gas switching within this short period. In quaternary $In_{0.58}Ga_{0.42}As_{0.9}P_{0.1}/InP$ quantum wells,[21] we reported that the interface quality is greatly improved by lowering the growth temperature below 570 °C. We think that this is another way to prevent the substitution. Improving the reactor design to enable fast gas switching and developing methods to prevent atomic substitution at interfaces, very smooth interface can be obtained also in $In_{0.53}Ga_{0.47}As/InP$ quantum wells.

Chemla studied the temperature dependence of the exciton spectrum width in a $GaAs/Al_{0.28}Ga_{0.72}As$ MQW, and fit Eqs. (12) and (13) to the experimental data using $\Gamma_0=4$ meV, $\hbar\omega_{LO}=36$ meV, and $\Gamma_{ph}=11$ meV.[17] The spectrum width at 295 K is calculated to be 7.5 meV. The broadening function B in our model gives the same spectrum width using $\Gamma_0=4$ meV and $\bar{\tau}=500$ fs at 295 K. We again assumed that $f(\tau)$ obeys a Lorentzian distribution with the FWHM of half the average. Using $\hbar\omega_{LO}=32$ meV and $\tau_{ph}=200$ fs in Eq. (22), the temperature dependence can be explained. The average lifetime of 300 fs at 295 K in $In_{0.53}Ga_{0.47}As/InP$ quantum wells is 60% of that in $GaAs/Al_{0.28}Ga_{0.72}As$ quantum wells. The thermal broadening is larger in $In_{0.53}Ga_{0.47}As/InP$ quantum wells primarily due to the larger exciton phonon coupling represented by τ_{ph}^{-1}. As a result, the room-temperature spectrum width of about 11 meV in sample I was much broader than that of 7.5 meV in $GaAs/Al_{0.28}Ga_{0.72}As$ quantum wells, though the two samples have nearly equal inhomogeneous broadening.

From the above discussion, we conclude that both the presence of composition fluctuations in $In_{0.53}Ga_{0.47}As$ wells and the larger exciton phonon coupling makes the exciton spectrum intrinsically broader in $In_{0.53}Ga_{0.47}As/InP$ quantum wells than in $GaAs/Al_{1-x}Ga_xAs$ quantum wells.

Equation (12) has been used to describe the temperature dependence of exciton spectrum width by other authors. This equation explained the measured temperature dependence quite well using LO phonon as the major scattering source. Weiner[22] has noticed that the contribution of thermal broadening in $In_{0.53}Ga_{0.47}As$ quantum wells is larger than that in GaAs quantum wells by comparing the parameter of Γ_{ph} in Eq. (13). (In Ref. 20, we discussed that the magnitude of thermal broadening is similar in both quantum wells. We admit that this result is based on our misunderstanding of the data presented by Chemla[17] and is incorrect.) His data on the temperature dependence (Fig. 2 in Ref. 22) are quite similar to those of sample III. It is interesting to note that our data and the calculated solid lines in Fig. 5 look as if some kind of broadening factor common in the three samples is summed to the inhomogeneous broadening. Thus, in the sense that we can estimate the exciton spectrum width from the inhomogeneous broadening by a very simple analytical calculation, Eqs. (12) and (13) are useful. We must note, however, that this is only an empirical equation and has no physical meaning. Thus, the relation between the excition lifetime and Γ_T is not clear. Using the uncertainty relation of $\bar{\tau}=\hbar/\Gamma_T$, Miller[8] and Chemla[17] calculated the average exciton lifetime to be about 400 fs in 10-nm $GaAs/Al_{0.28}Ga_{0.72}As$ quantum wells, and Weiner[22] calculated it to be 260 fs in $In_{0.53}Ga_{0.47}As/Al_{0.52}In_{0.48}As$ quantum wells. Surprisingly, these values coincide well with those we obtained despite the different methods of analysis. Recall that the broadening function due to the uncertainty $(1/\pi b)\sin^2(E/b)/(E/b)^2$ has a FWHM of $5.56\hbar/\tau$. Thus, they used an incorrect relationship between the width of broadening function and the average exciton lifetime. This is the reason for their similarity with our results.

Finally, we would like to comment on the electron-LH exciton resonance. From the 4.2- and 295-K spectra in Fig. 4, we can see that electron-LH exciton resonance is weaker than electron-HH exciton resonance. The peak absorbance decreases as temperature increases, probably due to the same thermal broadening mechanism as in the electron-HH excition resonance. To evaluate the spectra quantitatively, we need to precisely extract the contribution of electron-LH transition from the measured spectra. We did not do this procedure because it would cause fairly large errors. We can say that the integrated intensity is smaller primarily because $M_{QW}=\frac{1}{2}$ in Eq. (9) ($\frac{1}{3}$ the size in electron-HH transition) for the electron-LH transition. Other characteristics of excitons such as the two-dimensional radius, the effect of composition fluctuation, and the coupling constant with LO phonons will be slightly modified through the change in the reduced effective mass.

V. CONCLUSION

We studied exciton optical-absorption resonance in $In_{0.53}Ga_{0.47}As/InP$ quantum wells both theoretically and experimentally. We discussed the theoretical formula for the integrated intensity and the profile of exciton resonance spectrum. Based on our model, we analyzed the electron-HH exciton resonance spectrum in $In_{0.53}Ga_{0.47}As/InP$ quantum wells grown by MOVPE.

We presented a formula on the integrated intensity explicitly including the material parameters of quantum wells. The integrated intensity was experimentally determined to be 1.1×10^{-4} eV, which was about 70% of that in the $GaAs/Al_{0.25}Ga_{0.75}As$ quantum wells reported by Masselink.[31] The smaller integrated intensity is due to the larger two-dimensional exciton radius caused by the larger static dielectric constant and the smaller in-plane reduced effective mass.

We proposed that the profile of the exciton spectrum be formed by the convolution integral between the broadening function due to the spatial inhomogeneity of

exciton energy and that due to the reduction of the exciton lifetime by thermal phonon scattering. The inhomogeneous broadening function was found to be Gaussian at low temperatures. We could explain the room-temperature spectrum profile assuming that the distribution function of exciton lifetime is Lorentzian with a FWHM half the average. The average exciton lifetime was found to be 300 fs at 295 K. The temperature dependence of the spectrum width is explained by this model using LO phonons as the major source of exciton scattering. The exciton spectrum in $In_{0.53}Ga_{0.47}As/InP$ quantum wells is intrinsically broader than in $GaAs/Al_{1-x}Ga_xAs$ quantum wells due to composition fluctuation in $In_{0.53}Ga_{0.47}As$ wells and the larger exciton phonon coupling.

We conclude that $In_{0.53}Ga_{0.47}As/InP$ quantum wells intrinsically have weaker exciton resonance than $GaAs/Al_{1-x}Ga_xAs$ quantum wells. There is a key point to observe exciton resonance at room temperature in this quantum well: to limit the inhomogeneous broadening to below about 10 meV. Our three samples satisfied this condition, and showed room-temperature exciton resonance. The analysis used in this paper can also be used to study the exciton resonance in other quantum wells.

ACKNOWLEDGMENTS

We wish to thank Dr. T. Sakurai, Dr. H. Imai, K. Tanaka, and K. Domen for many helpful discussions leading to the preparation of this paper. We would also like to express heartfelt thanks to Miki Sugawara for her continuous encouragement.

[1]T. Ishibashi, S. Tarucha, and H. Okamoto, in Proceedings of the International Symposium on GaAs and Related Compounds, Oslo, 1981 [Inst. Phys. Conf. Ser. **63**, 587 (1981)].

[2]*Semiconductor and Semimetals* (Academic, New York, 1966), Vol. II, Chap. 6.

[3]R. L. Greene and K. K. Bajaj, Solid State Commun. **45**, 831 (1983).

[4]Y. Masumoto and M. Matsuura, Surf. Sci. **170**, 635 (1986).

[5]R. Dingle, Festkörperprobleme **15**, 21 (1975).

[6]G. Bastard and J. A. Brum, IEEE J. Quantum Electron. **QE-22**, 1625 (1986).

[7]D. A. B. Miller, D. S. Chemla, T. C. Damen, A. C. Gossard, W. Wiegmann, T. H. Wood, and C. A. Barrus, Phys. Rev B **32**, 1043 (1985).

[8]D. A. B. Miller, D. S. Chemla, D. J. Eilenberger, P. W. Smith, A. C. Gossard, and W. T. Tsang, Appl. Phys. Lett. **41**, 679 (1982).

[9]H. Haug and S. Schmitt-Rink, Prog. Quantum Electron. **9**, 3 (1984).

[10]H. Haug and S. Schmitt-Rink, J. Opt. Soc. Am. B **2**, 1135 (1985).

[11]S. Schmitt-Rink, D. S. Chemla, and D. A. B. Miller, Phys. Rev. B **32**, 6601 (1985).

[12]T. H. Wood, C. A. Burrus, D. A. B. Miller, D. S. Chemla, T. C. Damen, A. C. Gossard, and W. Wiegmann, Appl. Phys. Lett. **44**, 16 (1984).

[13]D. A. B. Miller, D. S. Chemla, T. C. Damen, A. C. Gossard, W. Wiegmann, T. H. Wood, and C. A. Burrus, Appl. Phys. Lett. **45**, 163 (1984).

[14]D. A. B. Miller, D. S. Chemla, T. C. Damen, T. H. Wood, C. A. Burrus, A. C. Gossard, and W. Wiegmann, IEEE J. Quantum Electron. **QE-21**, 1462 (1985).

[15]H. M. Gibbs, S. S. Tarng, J. L. Jewell, D. A. Weinbergar, K. Tai, A. C. Gossard, S. L. McCall, A. Passner, and W. Wiegmann, Appl. Phys. Lett. **41**, 221 (1982).

[16]S. Tarucha, and H. Okamoto, Appl. Phys. Lett. **49**, 543 (1986).

[17]D. S. Chemla, D. A. B. Miller, P. W. Smith, A. C. Gossard, and W. Wiegmann, IEEE J. Quantum Electron. **QE-20**, 265 (1984).

[18]H. Iwamura, H. Kobayashi, and H. Okamoto, Jpn. J. Appl. Phys. Pt. 2, **23**, L795 (1984).

[19]M. Sugawara, T. Fujii, M. Kondo, K. Kato, K. Domen, S. Yamazaki, and K. Nakajima, Appl. Phys. Lett. **53**, 2290 (1988).

[20]M. Sugawara, T. Fujii, M. Kondo, S. Yamazaki, and K. Nakajima, in Proceedings of the Fifteenth International Symposium on GaAs and Related Compounds, Atlanta, 1988 [Inst. Phys. Conf. Ser. **96**, 309 (1988)].

[21]M. Sugawara, T. Fujii, S. Yamazaki, and K. Nakajima, Appl. Phys. Lett. **54**, 1353 (1989).

[22]J. S. Weiner, D. S. Chemla, D. A. B. Miller, T. H. Wood, D. Sivco, and A. Y. Cho, Appl. Phys. Lett. **46**, 619 (1985).

[23]I. Bar-Joseph, C. Klingshirn, D. A. B. Miller, D. S. Chemla, U. Koren, and B. I. Miller, Appl. Phys. Lett. **50**, 1010 (1987).

[24]M. S. Skolnick, L. L. Taylor, S. J. Bass, A. D. Pitt, D. J. Mowbray, A. G. Cullis, and N. G. Chew, Appl. Phys. Lett. **51**, 24 (1987).

[25]H. Kamei, T. Katsuyama, K. Ono, and K. Yoshida, in Proceedings of the Fifteenth International Symposium on GaAs and Related Compounds, Atlanta, 1988 [Inst. Phys. Conf. Ser. **96**, 125 (1988)].

[26]W. Stolz, J. C. Maan, M. Altarelli, L. Tapfer, and K. Ploog, Phys. Rev. B **36**, 430 (1987).

[27]Y. Kawamura, K. Wakita, and H. Asahi, in Proceedings of the International Symposium on GaAs and Related Compounds, Karuizawa, 1985 [Inst. Phys. Conf. Ser. **79**, 451 (1986)].

[28]T. Miyazawa, S. Tarucha, S. Ohmori, Y. Suzuki, and H. Okamoto, Jpn. J. Appl. Phys. Pt. 2 **25**, L200 (1986).

[29]F. Bassani and C. P. Parravicini, *Electronic States and Optical Properties in Solids* (Pergamon, New York, 1975), Chap. 7.

[30]G. D. Sanders and Y. C. Chang, Phys. Rev. B **31**, 6892 (1985).

[31]W. T. Masselink, P. J. Pearah, J. Klem, C. K. Peng, H. Morkoc, G. D. Sanders, and Yia-Chung Chang, Phys. Rev. B **32**, 8027 (1985).

[32]D. F. Welch, G. W. Wicks, and L. E. Eastman, J. Appl. Phys. **55**, 3176 (1984).

[33]E. O. Kane, Phys. Chem. Solids **1**, 249 (1957).

[34]M. Yamanishi and I. Suemune, Jpn. J. Appl. Phys. Pt. 2 **23**, L35 (1984).

[35]G. Bastard, Phys. Rev. B **24**, 4714 (1981).

[36]J. Singh and K. K. Bajaj, Appl. Phys. Lett. **44**, 1075 (1984).

[37]J. Singh and K. K. Bajaj, J. Appl. Phys. **57**, 5433 (1985).

[38]J. Lee, E. S. Koteles, and M. O. Vassell, Phys. Rev. B **33**, 5512 (1986).

[39]Y. Kawaguchi and H. Asahi, Appl. Phys. Lett. **50**, 1243 (1987).

[40]L. I. Schiff, Quantum Mechanics (McGraw-Hill, New York, 1968).
[41]S.-C. Hong, G. P. Kothiyal, N. Debbar, P. Bhattacharya, and J. Singh, Phys. Rev. B **37**, 878 (1988).
[42]M. Shinada and S. Sugano, J. Phys. Soc. Jpn. **21**, 1936 (1966).
[43]M. Sugawara, M. Kondo, S. Yamazaki, and K. Nakajima, Appl. Phys. Lett. **52**, 742 (1988).
[44]M. Sugawara, M. Kondo, S. Yamazaki, and K. Nakajima, J. Cryst. Growth **93**, 318 (1988).
[45]S. R. Forrest, P. H. Schmidt, R. B. Wilson, and M. L. Kaplan, Appl. Phys. Lett. **45**, 1199 (1984).
[46]T. P. Pearsall, *GaInAsP Alloy Semiconductors* (Wiley, New York, 1982), p. 456.
[47]K. G. Hambleton, Proc. Phys. Soc. London **77**, 1147 (1961).
[48]K. Alavi, R. L. Aggarwal, and S. H. Groves, Phys. Rev. B **21**, 1311 (1980).
[49]W. Stolz, J. C. Maan, Altarelli, L. Tapfer, and K. Ploog, Phys. Rev. B **36**, 4310 (1987).
[50]R. K. Soni, S. C. Abbi, K. P. Jain, M. Balkanski, S. Slempkes, and J. L. Benchimol, J. Appl. Phys.**59**, 2184 (1986).
[51]E. F. Schubert, E. O. Gobel, Y. Horikoshi, K. Ploog, and H. J. Queisser, Phys. Rev. B **30**, 813 (1984).
[52]T. Y. Wang, E. H. Reihlen, H. R. Jen, and G. B. Stringfellow, J. Appl. Phys. **66**, 5376 (1989).